

Probabilistic Response Evaluation of Plan-Irregular Buildings Subjected to Bi-directional Seismic Loading

Salar Manie^{1*}, Abdoreza S. Moghadam², and Mohsen Ghafory-Ashtiany²

¹ Department of Civil Engineering, College of Engineering, Tehran Science and Research Branch, Islamic Azad University, Tehran, Iran

² International Institute of Earthquake Engineering & Seismology (IIEES), North Dibajee St., Farmanieh, Tehran, Iran

*Corresponding author's E-mail: salarmanie@srbiau.ac.ir

ABSTRACT: The present paper aim at evaluating the response of three-dimensional buildings with in-plan unidirectional mass irregularities subjected to bi-directional seismic loading. The study is carried out in a probabilistic frame-work considering the response of the structural models at their near-collapse nonlinear state of response. To this end, three-dimensional 3 and 6-story reinforced concrete building structures with unidirectional mass eccentricities equal to 0% (symmetrical), 10%, 20% and 30%, were subjected to extensive nonlinear incremental dynamic analyses (IDA) utilizing degrading hysteretic models under a set of far-field two-component ground motions records. The collapse-level intensities of each model under all records were, then, assessed using standard uni-variate as well as bi-variate statistical and probabilistic analysis procedures. Results demonstrated that remarkable differences exist between behavior of regular and irregular buildings in terms of median collapse-level spectral intensities, the corresponding coefficients of variation, and the properties of the associated probability density and cumulative density functions (PDFs and CDFs). The paper, also, introduces the "fragility surface" concept as an alternative to conventional fragility curves for collapse behavior assessment of three-dimensional structures.

Keywords: Torsional Buildings, Probabilistic, Collapse, Plan Irregularity, Low-Rise Buildings.

ORIGINAL ARTICLE
Received 21 Mar. 2014
Accepted 30 Apr. 2014

INTRODUCTION

Probabilistic seismic assessment procedures have proved to be an invaluable performance-based tool in modern earthquake engineering (Jalayer, 2003; Bozorgnia and Bertero, 2004). This is due to the fact that the seismic demands and the response of the structure as well are both probabilistic in nature. In previous studies (e.g. Jalayer, 2003; Ibarra et al., 2005; Haselton, 2006; Zareian and Medina, 2010), elements of rational probabilistic and statistical structural evaluation procedures under seismic loading have been established. In those studies, various aspects of the probabilistic structural evaluation procedures such as the way in which the hazard should be defined, the structural modeling and analyzing techniques in different phases of response from the elastic to highly inelastic and even the collapse states of response, performance criteria and etc. have been studied. Among all, establishment of performance criteria on the basis of collapse response of structures taking the post-peak descending branch of the response into consideration using nonlinear incremental dynamic analysis (IDA) and degrading nonlinear models is a major advancement in the field. Elements of such analysis have been discussed in detail in (Vamvatsikos and Cornell, 2001). In this regard, FEMA-P695 (FEMA, 2009) serves as a document which provides recommendations for collapse response assessment of structures from a probabilistic point of view. The document contains almost all the critical research outputs in the field up to the date of publication and is

intended to assess the safety margin of structures against collapse (collapse-level capacity) as well as to provide a methodology for evaluating the assumed initial seismic design parameters in a probabilistic framework. The proposed methodology in that document is entirely based on pushover analysis as well as nonlinear IDA results under a set of far-field and/or near-field strong ground motions.

Irregularity conditions in plan, on the other hand, may arise due to large distance between the center of mass (CM) and the center of stiffness (CR) in the elastic (pre-yielding) range of response, or the center of mass (CM) and the center of strength (CV) in the post-yielding range of response. In the past seismic events, inappropriate response of torsional structures has been one of the most important causes of structural failures and fatalities (Fardis, 2009). In these structures, the distribution of seismic demands in the structure is not uniform and the displacement and ductility demands on the elements along the so-called "stiff side" are generally different from those on the "soft (flexible) side" (Paulay, 2001; Wong and Tso, 1994; Paulay and Priestly; 1992, Chopra, 2008). Due to the strong dynamic coupling of torsional and translational effects, the performance of such structures is basically different from the structures in which these effects are minimal. Response of torsional structures due to the coupling effects is affected by various parameters and is generally accompanied by high levels of uncertainties. Thus, probabilistic evaluation of such structures will certainly provide a better insight into their performance.

In previous studies, response of structures has been evaluated from the probabilistic point of view. Especially, regarding the collapse region of nonlinear response, two-dimensional (2D) frame structures have been studied probabilistically (e.g. Goulet et al., 2007; Haselton et al., 2011; Liel et al., 2011). Also, studies have been conducted on probabilistic collapse response of structures with irregularities in elevation (e.g. Varadharajan et al., 2012). In contrast, not so much research could be found in literature for probabilistic collapse assessment of three dimensional (3D) structures, particularly the torsional (irregular in plan) ones. Recently, DeBock et al. (2013) have investigated the effect of accidental torsional code requirements on collapse behavior of 3D structures using simplified models.

The present study is an attempt to evaluate the near collapse seismic response of low-rise 3D reinforced concrete (RC) frame buildings with mass irregularities in plan and under the simultaneous effects of both horizontal components of strong ground motions from a probabilistic point of view. To this end, three- and six-story RC models with uni-directional mass irregularities equal to 0% (symmetrical), 10%, 20% and 30%, and designed based on current seismic design code regulations according to high-ductility design and detailing requirements, have been subjected to extensive nonlinear incremental dynamic analyses (IDA) by simultaneous consideration of both horizontal ground motion components and their response have been assessed based on the adopted probabilistic approach of FEMA-P695 (FEMA, 2009). For performing the IDAs, 21 normalized records selected from the far-field records set of FEMA-P695 were utilized. Performance of each structure was, then, evaluated through assessment of IDA curves and their median curves, probability density functions (PDFs) and cumulative density functions (CDFs) of each structural model considering the collapse-level intensity points. Since the response of the structures are coupled in both directions, (especially at high levels of ground motion intensities), bi-variate probabilistic analysis have also been carried out along with the conventional uni-variate analysis techniques to quantify the inherent characteristics of nonlinear response of such structures near the collapse state.

MATERIAL AND METHODS

General specifications of the structural models

For the purposes of this study, 3 and 6-story RC buildings with typical architectural characteristics, as shown in Figure 1, are considered. All buildings are 3-story and 3-span by 3-span reinforced concrete moment frames designed based on ASCE/SEI 7-10 (ASCE, 2010) provisions. Reinforcements detailing conforms to the ACI code (ACI, 2011) requirements for "special moment resisting frames". Span lengths are identical in both directions equal to 5 meters and story heights are considered to be 3 meters. Distributed dead and live loads on floors are 5.3 KN/m² and 2 KN/m², respectively. It is assumed that all structures are located in a "high seismicity" area with the underlying soil being as "firm soil" based on ASCE/SEI 7-10 classification. 28-day concrete cylindrical specified strength and rebar

strength are assumed to be 30 MPa and 400 MPa, respectively. In the analysis and design processes, all lateral displacement limitations and strength requirements as mandated by ASCE/SEI 7-10 have been checked.

Nonlinear structural models

As discussed in FEMA P-695 (FEMA, 2009), Haselton (2006) and Ibarra et al. (2005), a monotonic curve for RC frame elements as shown in (Figure 2) could be utilized for modeling RC framed structures incorporating two nonlinear concentrated springs at the two ends of each element. All sources of strength and stiffness degrading effects are, then, lumped at these springs by incorporation of an appropriate plasticity model. The middle parts of all frame elements are assumed to remain elastic in all phases of response. Ibarra et al. (2005) proposed a hysteretic model, based on the kinematic hardening rules, applicable for nonlinear modeling of RC structures to assess their collapse behavior. The utilized hysteretic model in this study is known as "peak-oriented hysteretic model" and is depicted in Figure 3.

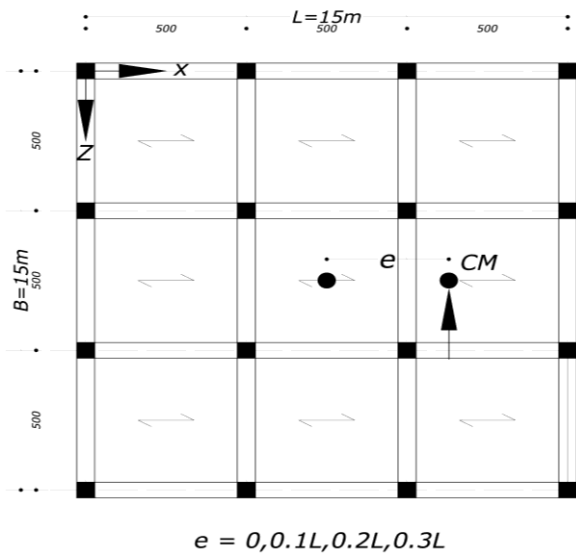


Figure 1. Typical stories plan

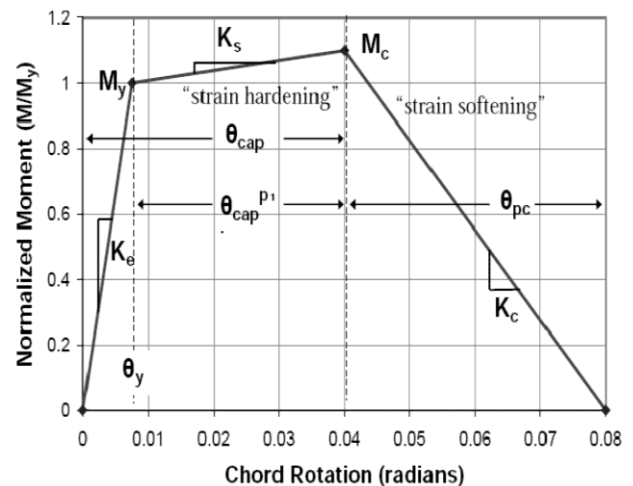


Figure 2. Monotonic behavior of an RC component (Ibarra et al., 2005)

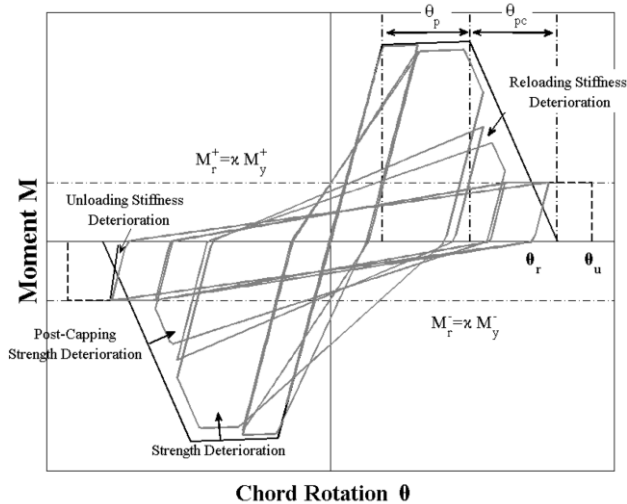


Figure 3. Hysteretic response of RC elements with stiffness and strength degradation (Ibarra et al., 2005)

Elastic analyses of all models were performed using appropriate cracked section properties on the basis of the recommendations outlined in FEMA P-695. Properties of the concentrated hinges including yield rotation and moment, plastic rotation capacity, post-yield rotation capacity, energy dissipation capacity per cycle of inelastic response, etc. have been calculated according to the recommended equations in Panagiotakos and Fardis (2001) using a computer program designed specifically for this purpose (Manie and Moghadam, 2012). Geometric nonlinearities including the global P- Δ as well as the local p-delta effects were considered in the modeling and analyzing processes. Mass properties of all structures were modeled using concentrated mass elements at the nodes. For mass eccentricities of 10% to 30%, nodal masses were assigned in such a way that the desired mass eccentricity could be achieved. Damping properties of all models were considered as of Rayleigh mass and stiffness proportional type based on the recommendations in Zareian and Medina (2010) for collapse behavior assessment of structure.

According to FEMA-P695, explicit modeling of beam-column joints and bar-slip effects are not necessary for modeling RC frames to perform collapse analyses, since all nonlinear elements specifications including the yield angle moment, cap angle and moment, ultimate angle, etc. are based on regression analysis of real tests. Discussion on modeling beam-column joints considering the bar-slip effects can be found elsewhere (e.g. Moridani and Zarfam).

Analytical methods

For the purposes of this study, all buildings models were subjected to bidirectional nonlinear incremental dynamic analyses (IDAs) (Vamvatsikos and Cornell, 2001). Then, responses of all models were evaluated at the center of mass (CM), the stiff and the flexible sides of the plan. Incremental dynamic analyses were performed using a set of far-field records including 21 pairs of horizontal ground motions introduced in FEMA P-695 for collapse level analyses. In Figure 4, the median pseudo-acceleration spectrum of all records and the MCE design spectrum are shown.

In fact, the collapse safety of structures should be assessed in a statistical and probabilistic framework using results of incremental nonlinear time-history analyses. In the method adopted in FEMA-P695, each record is scaled-up at the spectral intensity corresponding to the fundamental mode of the structure in the direction of interest on the median response spectrum of all records. The scale factor, SF , should be computed for both horizontal directions and the average value be used to scale both components of each record. Scaling-up is continued until a global collapse state or other limit states are reached.

Due to the high number of nonlinear analysis runs (with the total number of 3500 for each structure of 0 to 30% mass eccentricity values), the Multi-frontal Massively Parallel Sparse Direct Solver (Mumps) algorithm (OpenSees, 2006) was utilized for solving the large systems of nonlinear equations usually encountered in three-dimensional nonlinear analysis. The "Mumps" algorithm has been implemented in the parallel version of OpenSees simulation platform (OpenSees, 2006). In all the analyses, the Newmark integration scheme (Chopra, 2008) was utilized. The collapse level spectral intensities of all records are, then, utilized to perform all probabilistic calculations.

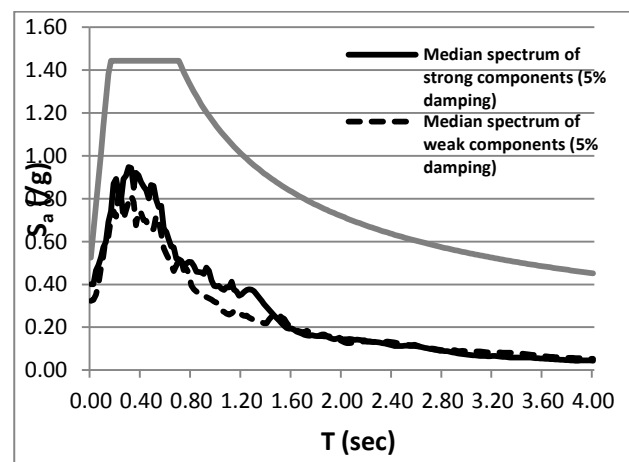


Figure 4. Median spectrum of strong and weak components of records with the design MCE level spectrum

RESULTS

In this section, the results of nonlinear incremental time-history analyses and the associated probabilistic calculations are presented for the models with different plan eccentricities from 0 to 30%, separately. These results include the IDA curves and their median curves, collapse-level spectral intensities, probability density functions (PDFs) and cumulative density functions (CDFs) of each structural model separately, all calculated from the incremental dynamic analysis of nonlinear models. Also, probabilistic analyses will be carried out on each model using univariate and bi-variate analysis techniques.

Incremental dynamic analyses results

In this study, three distinct criteria, as mentioned below, have been used to identify the spectral intensity

corresponding to the collapse state of the building models in each direction:

1) Spectral intensity corresponding to a maximum drift value equal to 10% wherever in the structure on the IDA curves,

2) Spectral intensity corresponding to the flattening of IDA curves, and,

3) Spectral intensity corresponding to reaching a specific limit state in the elements of the structure; for example, the shear failure of one or more columns.

The least of (1) to (3) was considered as the collapse capacity of buildings under the effect of each record. Since three-dimensional nonlinear models have been used for all buildings, all IDA analyses have been performed by applying simultaneous horizontal components of ground motions.

Figures 5-a, 5-b depict typical results of IDAs for the symmetrical (eccentricity equal to 0%) three-story

model. IDA curves have been drawn as the spectral intensity at the fundamental mode of the structure in the direction of interest vs. the maximum inter-story drift observed in that direction for each ground motion of increasing intensity along with their median curve. Performance of building models are evaluated using the median curves. Tables 1 and 2 show the collapse-level spectral intensities of all 8 nonlinear models of 3 and 6-story buildings for each plan direction and for each value of plan mass eccentricity ratio (ECC), separately. Note that, the values shown in these tables are reported directly from nonlinear incremental dynamic analyses without applying adjusting factors outlined in FEMA-P695 for spectral shape and 3D effects. For our discussion, these factors need not be considered. Corresponding statistical parameters have also been calculated at the end of the tables for each model, separately.

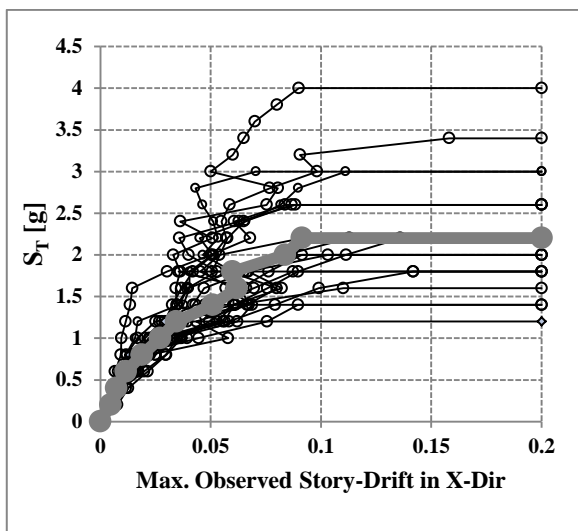


Figure 5a. IDA curves with the median curve (3-story model; X-Dir; ECC: 0%)

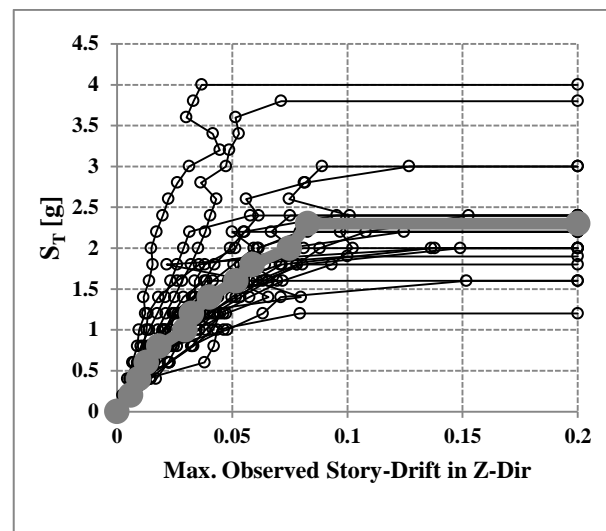


Figure 5b. IDA curves with the median curve (3-story model; Z-Dir; ECC: 0%)

Table 1. Non-adjusted (Raw) collapse-level spectral intensities for the 3-story model with the associated statistical parameters

Record No.	ECC: 0% (Sym.)		ECC: 10%		ECC: 20%		ECC: 30%	
	X-dir $\hat{S}_{CT-X/g}$	Z-dir $\hat{S}_{CT-Z/g}$	X-dir $\hat{S}_{CT-X/g}$	Z-dir $\hat{S}_{CT-Z/g}$	X-dir $\hat{S}_{CT-X/g}$	Z-dir $\hat{S}_{CT-Z/g}$	X-dir $\hat{S}_{CT-X/g}$	Z-dir $\hat{S}_{CT-Z/g}$
1	2.20	2.06	2.52	1.63	2.20	1.10	1.64	0.76
2	2.18	2.24	1.55	2.12	1.40	2.19	1.82	1.86
3	1.80	2.06	1.57	1.63	1.39	1.85	1.27	1.86
4	3.00	2.80	2.50	1.79	2.19	1.52	2.18	2.03
5	1.40	0.80	2.13	1.14	1.60	1.43	1.63	1.10
6	1.81	2.06	1.75	1.63	1.59	1.94	1.46	1.19
7	1.79	1.87	1.36	1.63	1.61	0.84	1.63	1.53
8	3.40	1.68	2.72	1.63	1.80	1.35	2.36	1.19
9	1.61	2.24	1.56	1.96	1.62	1.52	1.45	1.69
10	2.00	3.74	1.94	3.10	1.78	2.70	1.62	2.37
11	2.61	1.20	3.69	1.30	2.40	1.10	2.37	1.53
12	4.00	2.24	2.04	3.10	3.20	2.19	1.82	1.19
13	2.21	2.24	1.84	2.12	2.00	2.87	1.81	2.03
14	1.99	2.24	1.16	2.28	1.40	1.94	0.91	2.03
15	1.39	2.06	1.97	1.63	1.21	2.36	1.09	2.37
16	2.00	1.40	2.11	3.34	1.59	2.19	1.28	1.53
17	2.61	2.00	2.51	1.63	1.81	1.18	2.17	0.68
18	2.59	2.00	2.10	2.61	1.79	1.52	1.84	1.53
19	1.20	2.80	2.31	1.47	2.16	2.36	2.18	1.86
20	3.05	2.50	2.14	2.93	2.05	1.52	1.64	1.19
21	2.05	4.00	1.96	2.28	1.38	2.70	1.10	1.19
Median	2.05	2.06	2.04	1.79	1.78	1.85	1.64	1.53
Mean	2.23	2.25	2.07	2.04	1.82	1.82	1.68	1.55
Standard Deviation (SD)	0.7	0.73	0.55	0.64	0.45	0.59	0.42	0.48
Coefficient of Variation (COV)	0.31	0.33	0.26	0.31	0.25	0.33	0.25	0.31

Table 2. Non-adjusted (Raw) spectral intensities for the 6-story model with the associated statistical parameters

Record No.	ECC: 0% (Sym.)		ECC: 10%		ECC: 20%		ECC: 30%	
	X-dir $\hat{S}_{CT-X/g}$	Z-dir $\hat{S}_{CT-Z/g}$	X-dir $\hat{S}_{CT-X/g}$	Z-dir $\hat{S}_{CT-Z/g}$	X-dir $\hat{S}_{CT-X/g}$	Z-dir $\hat{S}_{CT-Z/g}$	X-dir $\hat{S}_{CT-X/g}$	Z-dir $\hat{S}_{CT-Z/g}$
1	2.32	2.00	1.54	1.36	0.81	0.84	0.65	0.63
2	1.89	1.64	1.76	1.62	1.22	1.26	0.64	0.65
3	1.91	1.63	2.00	2.18	1.42	1.48	1.05	1.12
4	1.05	0.91	1.76	1.45	1.23	1.25	1.03	0.80
5	0.84	0.73	2.20	1.82	2.03	1.90	0.79	0.48
6	1.26	1.09	1.10	0.92	0.81	0.86	0.77	0.49
7	1.47	1.46	1.32	1.65	1.12	1.24	1.04	0.64
8	1.68	1.45	1.97	0.90	1.63	1.69	1.56	0.96
9	1.05	1.00	0.89	1.20	0.81	1.10	1.00	1.12
10	1.08	0.82	1.16	1.20	1.02	1.20	1.31	1.11
11	1.24	1.11	0.88	0.74	1.12	0.37	0.91	0.57
12	2.32	2.02	1.54	1.05	1.63	0.60	0.78	0.49
13	1.08	0.94	1.12	0.40	0.81	1.50	1.06	1.50
14	1.25	1.13	1.31	1.00	1.22	1.69	1.01	1.14
15	1.08	1.07	1.14	1.46	0.82	1.00	0.94	1.00
16	1.48	1.46	1.15	1.12	0.80	0.60	0.79	0.96
17	1.03	0.60	1.07	1.00	1.63	1.00	0.82	1.29
18	1.28	0.71	1.33	1.10	1.12	0.60	1.03	0.66
19	1.92	0.50	1.77	1.20	1.04	0.60	1.60	0.96
20	0.84	0.93	0.88	0.71	1.25	0.87	0.84	0.65
21	2.35	1.98	2.00	0.70	2.25	1.00	1.82	0.45
Median	1.26	1.09	1.32	1.12	1.12	1.00	1.00	0.80
Mean	1.45	1.20	1.42	1.18	1.23	1.10	1.02	0.84
Standard Deviation (SD)	0.49	0.46	0.43	0.42	0.41	0.39	0.31	0.44
Coefficient of Variation (COV)	0.34	0.39	0.30	0.36	0.33	0.35	0.31	0.36

In figures (6a) and (6b), plots of (non-adjusted) median collapse-level spectral intensities and in figures (7a) and (7b) the corresponding coefficients of variation (COV) are depicted vs. plan eccentricity ratios for the 3 and 6-story models. It can be shown in figures (6a) and (6b) that the median collapse capacity of structures tends to decrease as the plan eccentricity increases. Figures (7a) and (7b) indicate that the COVs of the collapse-level intensities has general trend of reduction with the increase of number of stories and plan eccentricity ratios. These findings are also evident from tables 1 and 2. Thus, with the increase in plan eccentricity ratio, vulnerability of the buildings against collapse (in terms of reduction in collapse-level capacity) tends to increase, and in critical cases (typically for eccentricity values over 20%), the performance of the structure could be unacceptable according to the evaluation provisions adopted in FEMA-P695. Discussions on these findings will be provided in the following section.

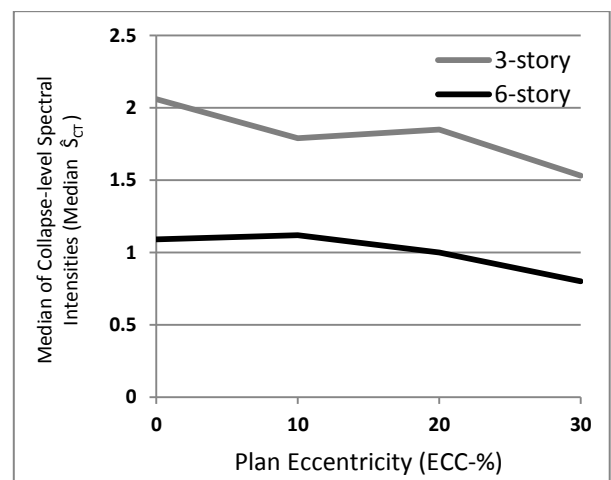


Figure 6b. Median of collapse spectral intensities (\hat{S}_{CT}) vs. plan eccentricity ratio for 3 and 6-story models (Z direction)

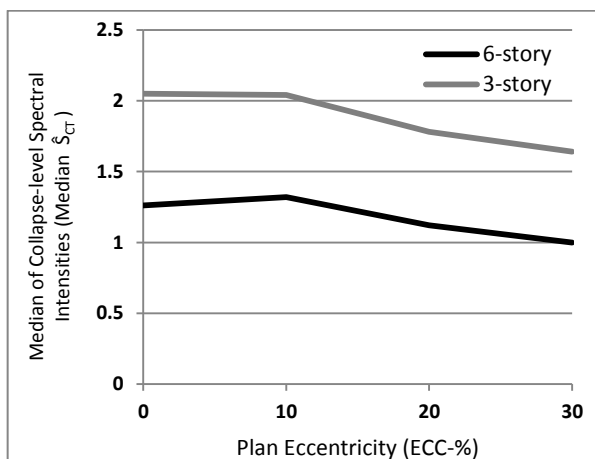


Figure 6a. Median of collapse spectral intensities (\hat{S}_{CT}) vs. plan eccentricity ratio for 3 and 6-story models (X direction)

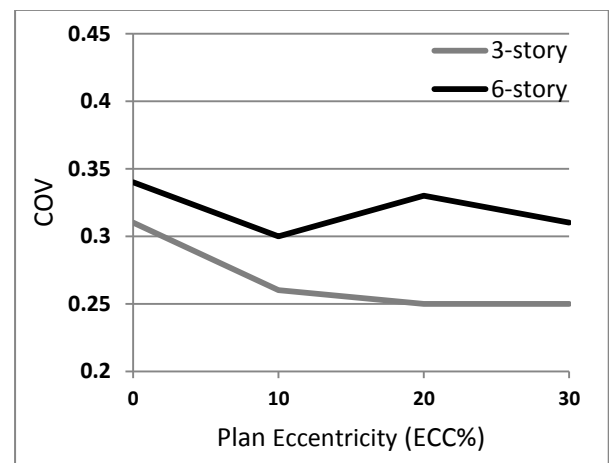


Figure 7a. Comparison of COV values for 3 and 6-story models (X direction)

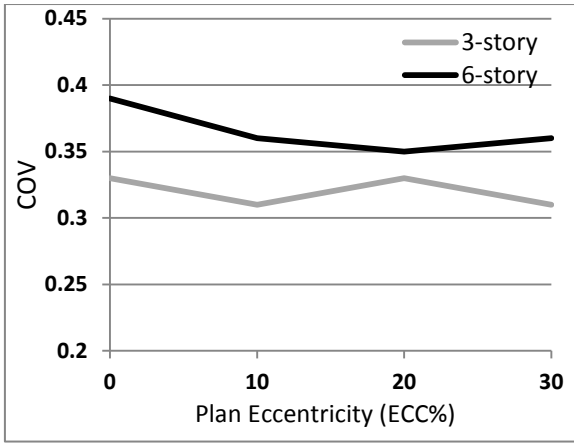


Figure 7b. Comparison of COV values for 3 and 6-story models (Z direction)

Figures 8 and 9 depict the cumulative density functions (CDFs) of collapse data points (termed as fragility curves in structural applications) derived for each building model via fitting a lognormal distribution (FEMA P-695) to the collapse-level intensities (21 data points corresponding to each record) extracted from the IDA curves. The curves represent the probability of collapse conditioned on a specific value of ground motion spectral intensity $S_{ax} = x$ or $S_{az} = z$ (S_{ax} stands for the spectral intensity in the X-direction, while S_{az} stands for the spectral intensity in the Z-direction at the fundamental mode of the structure) in the direction of interest; i.e. $P_{collapse} | S_{ax} = x$ or $P_{collapse} | S_{az} = z$. In these figures, CDFs have been drawn for both x and z directions, separately. Typically, the collapse capacity of structure is evaluated at the 50% level of probability on these curves (FEMA P-695, 2009).

The slope of the curves is an indicator of the uncertainties associated with the collapse-level capacities. Generally, fragility curves are flatter for buildings with high degrees of uncertainty in response (FEMA P-695) compared with structures in which uncertainties in their response are lower. Changes in the shape of the curves are evident for buildings with plan eccentricity of 20% and more, especially in the X direction of the plan. Discussion of the results will be covered in the next section.

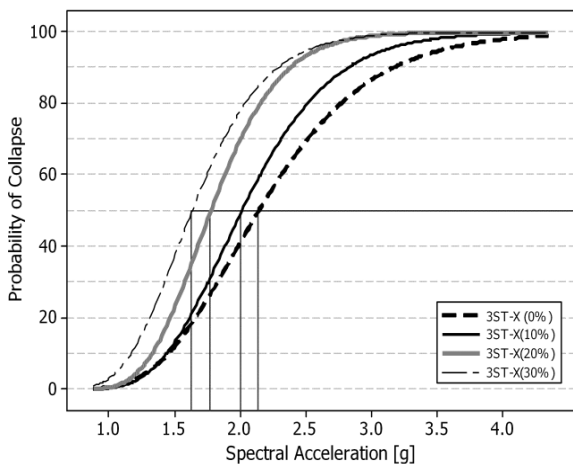


Figure 8a. CDFs (Fragility curves) for the 3-story model with different eccentricities (X-direction)

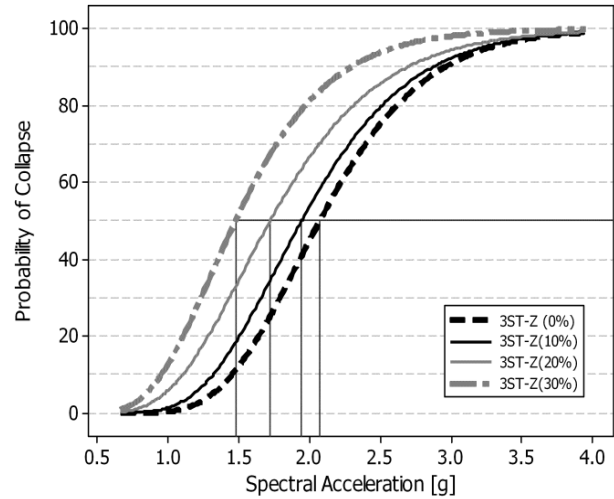


Figure 8b. CDFs (Fragility curves) for the 3-story model with different eccentricities (Z-Direction)

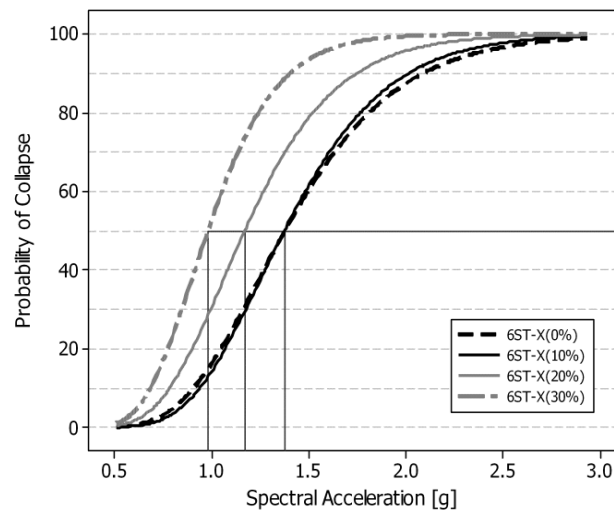


Figure 9a. CDFs (Fragility curves) for the 6-story model with different eccentricities (X-direction)

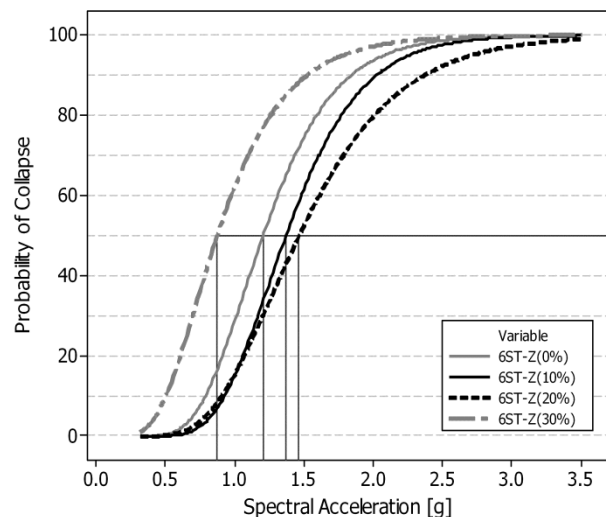


Figure 9b. CDFs (Fragility curves) for the 6-story model with different eccentricities (Z-direction)

Probabilistic assessment of 3D structures could also be investigated utilizing bi-variate probability density functions (PDFs) as well as bivariate cumulative density functions (CDFs). The latter is more useful in

assessing 3D structures, since the bi-variate CDF are essentially the fragility surface of the structure under the simultaneous effects of bi-directional ground motions, i.e. simultaneous application of S_{ax} and S_{az} . Fragility surfaces are introduced in this study as an alternative tool to fragility curves for collapse assessment of 3D structures under the simultaneous effects of both components of ground motions. In fact, a bi-variate CDF represents the probability of collapse conditioned on a specific pair of ground motion spectral intensities in both plan directions of the structure, i.e. $P_{collapse}(S_{ax} = x, S_{az} = z)$. Figures 10 and 11 show the bi-variate CDFs (fragility surfaces) of the 3 and 6-story models with different plan eccentricity ratios represented as contour plots. Contour plots seem to be interpreted more conveniently than their corresponding three-dimensional surfaces for our purposes. All pairs of $S_{ax} = x$ and $S_{az} = z$ on a specific curve (for example, the curve corresponding to 50% probability of collapse) exert the same hazard on the structure. Discussions on the plots will be provided in the next section.

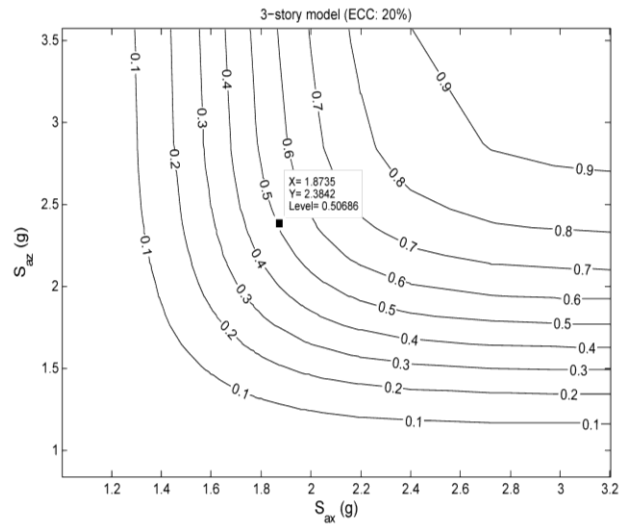


Figure 10c. Bi-variate CDF (fragility contours) for the 3-story model (ECC: 20%)

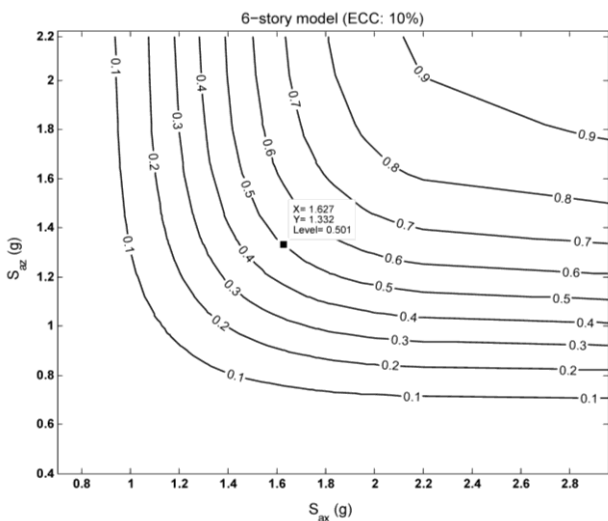


Figure 11b. Bi-variate CDF (fragility contours) for the 6-story model (ECC: 10%)

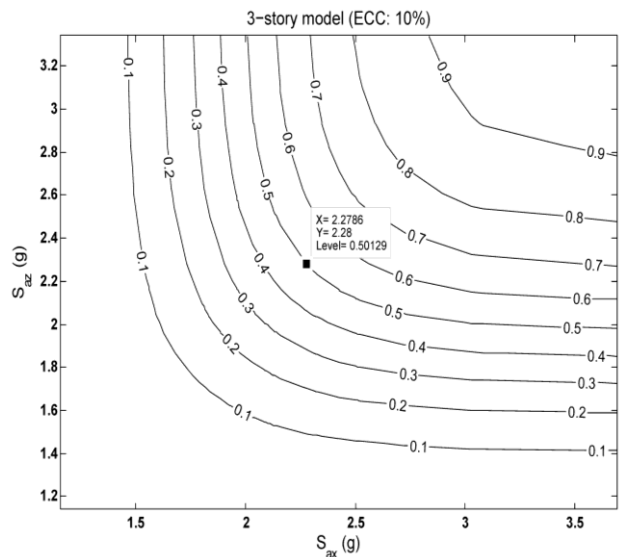


Figure 10b. Bi-variate CDF (fragility contours) for the 3-story model (ECC: 10%)

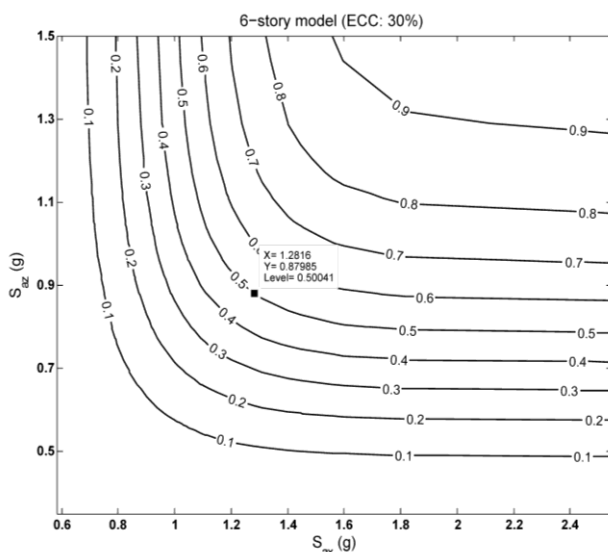


Figure 11d. Bi-variate CDF (fragility contours) for the 6-story model (ECC: 30%)

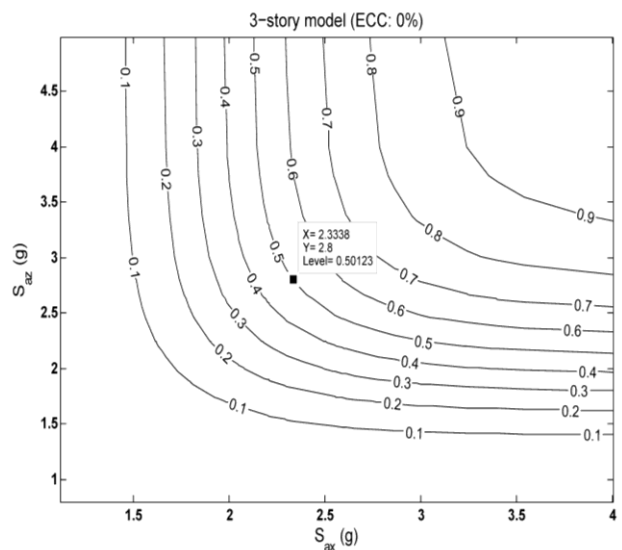


Figure 10a. Bi-variate CDF (fragility contours) for the 3-story model (ECC: 0%)

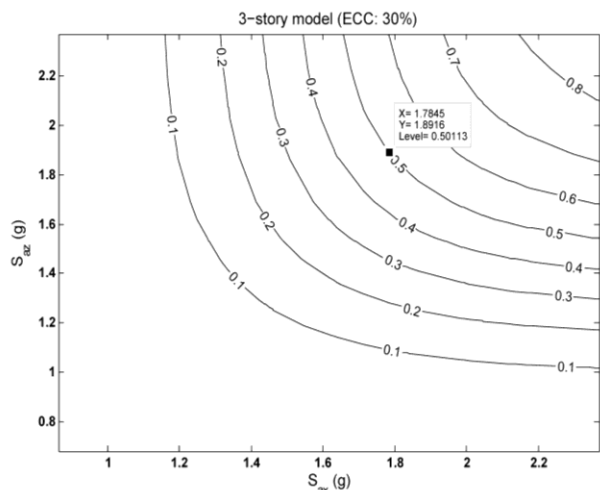


Figure 10d. Bi-variate CDF (fragility contours) for the 3-story model (ECC: 30%)

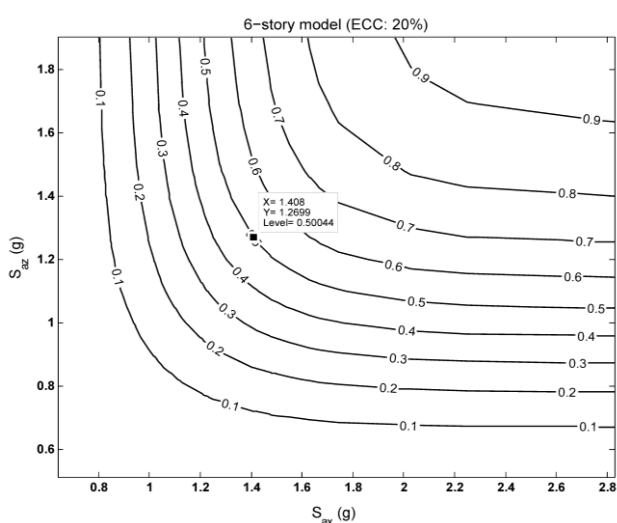


Figure 11c. Bi-variate CDF (fragility contours) for the 6-story model (ECC: 20%)

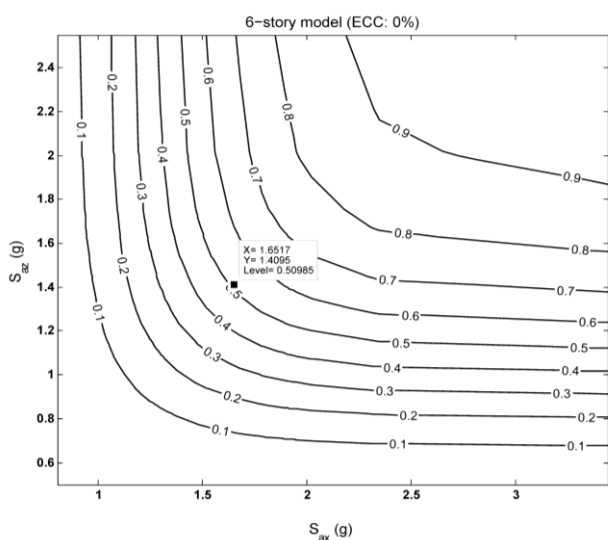


Figure 11a. Bi-variate CDF (fragility contours) for the 6-story model (ECC: 0%)

DISCUSSION

Examination of the probabilistic and statistical analyses presented above indicates that in low-rise

buildings with the increase of plan eccentricity, the lateral load capacity (considered in this study as the collapse-level spectral intensity of the structure) and the maximum tolerable inter-story drift are typically reduced in both directions of the plan. Comparison of the collapse spectral intensities in both directions (\hat{S}_{CT}) in tables 1 and 2, figure 6a, b shows that generally in all models \hat{S}_{CT} reduces with the increase of eccentricity in plan. The reductions are very substantial for buildings with plan eccentricities over 10%. Evaluation of figure 7a,b suggest that the coefficient of variation (COV) of the collapse spectral intensities tend to decrease as the plan eccentricity increases. As discussed in previous studies (e.g. Jalayer, 2003; Haselton 2006), the primary source of variation in nonlinear responses of structures near the collapse state of response is the “record-to-record (RTR)” variability among all other sources including the quality of nonlinear modeling, the quality of the test data, and the design and detailing requirements. Thus, the reduction in COV values with increasing the plan eccentricity ratios implies that by increasing the irregularity of the structure, the RTR variability of the response decreases and the properties of the structural model are more effective for the variability of the responses. This phenomenon is a very important finding of this study and could affect the seismic design provisions in design codes.

The fragility curves in figures 8 and 9 provide a very good tool for probability-based assessment of the collapse behavior of torsional buildings. As stated previously, typically, the collapse point is chosen to be the point with 50% probability of occurrence on the calculated fragility curve for the structure. Thus, as can be seen from those figures, movement of fragility curves from right to left with the increase in plan eccentricity could be attributed to the reduction in collapse capacity. Such reduction is quite pronounced for buildings with plan eccentricity over 10%.

Plan irregularity has affected the fragility curves especially in the plan “Z” direction (i.e. the direction perpendicular to the direction of plan eccentricity). Moreover, as the eccentricity value increases, the slope of the fragility curve increases. The increase in the slope of the curves is attributed to the reduction of the total uncertainty, which is consistent with the discussion on the COV values in the preceding paragraphs. Thus, the nonlinear structural characteristics are believed to be more dominant on the way that irregular buildings respond under sever seismic attacks. It is noted that in some cases (e.g. for the 6-story model with eccentricity ratio over 20%), the reduction in the collapse-level intensity on the fragility curve is so remarkable that the structure could not satisfy the design “life-safety” target performance level based on provisions of FEMA P-695. These issues will not be covered here, since the primary purpose of this study is to represent a comparative study of the response of in-plan irregular structures from probabilistic point of view.

Also, for 3D structures, fragility surfaces -as shown in figures 10 and 11 could be derived as an alternative to conventional fragility curves used in previous studies. In fact, fragility surfaces imply that various pairs of bi-directional ground motion intensities could expose the structure to a specific probability of

collapse. Examination of the bi-directional fragility contours shows that by increasing the plan mass eccentricity ratio as well as with the increase of the number of stories, vulnerability of the structure to collapse increases. This finding is in agreement with discussions made in the previous paragraphs.

It is believed that fragility surfaces-generated in the way discussed in this paper- could be an alternative tool for performance-based assessment of 3D structures under bi-directional seismic loadings.

CONCLUSION

The results of the statistical and probabilistic analyses of 3D structures demonstrate that collapse response of torsional low-rise buildings could be quite different in comparison to their non-torsional counterparts. Differences are quite evident from the collapse spectral intensities in both directions (\hat{S}_{CT}) of the plan as well as from the fragility curves and fragility surfaces. Statistical evaluation of nonlinear collapse analyses results indicate that as the amount of plan mass eccentricity increases, the collapse capacity of the building reduces. The study demonstrates that the variation in response of 3D structures decreases as the plan irregularity of the structure increases. Also, structure-specific fragility surfaces were introduced as an appropriate performance-check tool for seismic design of 3D structures incorporating both horizontal components of strong ground motion.

REFERENCES

ACI. (2011). Building Code Requirements for Structural Concrete (ACI 318-11) and Commentary, (ACI 318R-11), American concrete Institute, Farmington Hills, Michigan.

ASCE. (2010). Minimum Design Loads for Buildings and Other Structures, ASCE Standard ASCE/SEI 7-05, American Society of Civil Engineers, Reston Virginia.

Chopra AK. (2008). Dynamics of Structures: Theory and applications to earthquake engineering". 3rd Edition, Prentice-Hall of India.

DeBock D, Liel A, Haselton CB, Hooper J, Henige R. (2013). Importance of seismic design accidental torsion requirements for building collapse capacity. *Earthquake Engineering & Structural Dynamics*, 43(6): 831-850.

Fardis MN (Editor). (2009). Seismic design, assessment and retrofitting of concrete buildings based on EN-Eurocode 8. Springer.

FEMA. (2009). Quantification of Building Seismic Performance Factors, Report No. FEMA P695, Federal Emergency Management Agency, Washington, D.C.

Goulet CA, Haselton CB, Mitrani-Reiser J, Beck JL, Deierlein GG, Porter KA, Stewart JP. (2007). Evaluation of the seismic performance of a code-conforming reinforced-concrete frame building- From seismic hazard to collapse safety and economic losses. *Earthquake Engineering and structural dynamics*. 36(13): 1973-1997.

Haselton CB. (2006). Assessing Seismic Collapse Safety of Modern Reinforced concrete Moment-Frame Buildings, Ph.D. Dissertation, Department of Civil and Environmental Engineering, Stanford University, Stanford, California.

Haselton CB, Baker JW, Liel AB, Deierlein GG. (2011a). Accounting for ground-motion spectral shape characteristics in structural collapse assessment through an adjustment for epsilon." *J. Structural Engineering*, 137(3), 332-344.

Haselton CB, Liel A, Deierlein GG, Dean B, Chou J. (2011). Seismic Collapse Safety of Reinforced Concrete Buildings. I: Assessment of Ductile Moment Frames." *J. Struct. Eng.*, 137(4), 481-491.

Ibarra LF, Medina RA, Krawinkler H. (2005). "Hysteretic models that incorporate strength and stiffness deterioration." *International Journal for Earthquake Engineering and Structural Dynamics*, Vol. 34, No.12, pp. 1489-1511.

Jalayer F. (2003). Direct probabilistic seismic analysis: implementing nonlinear dynamic assessments, Ph.D. Dissertation, Department of Civil and Environmental Engineering, Stanford University, Stanford, California.

Karimi Moridani K, Zarfam P. (2013). Nonlinear Analysis of Reinforced Concrete Joints with Bond-Slip Effect Consideration in OpenSees. *Journal of Civil Engineering and Urbanism*, 3(6): 362-367.

Liel A, Haselton CB, Deierlein GG. (2011). Seismic Collapse Safety of Reinforced Concrete Buildings. II: Comparative Assessment of Non-ductile and Ductile Moment Frames. *Journal of Structural Engineering*, 137(4), 492-502.

Manie S, Moghadam AS. (2012). Experiences acquired through nonlinear modeling for collapse safety assessment of 3D RC structures with irregularities in plan. *Proceedings of 15th World Conference on Earthquake Engineering*, Lisbon, Portugal.

OpenSees. (2006). Open System for Earthquake Engineering Simulation, Pacific Earthquake Engineering research Center, University of California, available at <http://opensees.berkeley.edu>.

Paulay T, Priestley MJN. (1992). *Seismic Design of Reinforced Concrete and Masonry Buildings*. John Wiley & Sons.

Paulay T. (2001). Some Design Principles relevant to Torsional Phenomena in Ductile Buildings. *Journal of Earthquake Engineering*, 5:3, 273-308.

Panagiotakos TB, Fardis MN. (2001). Deformation of reinforced concrete members at yield and ultimate. *ACI Structural Journal*, 98 (2).

Varadharajan S, Sehgal V, Saini B. (2012). Seismic response of multistory reinforced concrete frame with vertical mass and stiffness irregularities. *The Structural Design of Tall and Special Buildings* 23(5): 362-389.

Vamvatsikos D, Cornell CA. (2001). Tracing and post-processing of IDA curves: Theory and software implementation, Report No. RMS-44, RMS Program, Stanford University, Stanford.

Wong CM, Tso WK. (1994). Inelastic seismic response of torsionally unbalanced systems designed using

elastic dynamic analysis. *Earthquake Engineering and Structural Dynamics*, 23, 7, pp. 777-79.

Zareian F, Medina RA. (2010). A practical method for proper modeling of structural damping in inelastic plane structural systems. *Journal of Computers and Structures*, 88, 45-53.